Impedance analysis of a radio-frequency single-electron transistor

H. D. Cheong,[a)] T. Fujisawa,[b)] T. Hayashi, and Y. Hirayama[c)]
NTT Basic Research Laboratories, NTT Corporation, 3-1 Morinosato-Wakamiya, Atsugi 243-0198, Japan

Y. H. Jeong
Department of Electronic and Electrical Engineering, Pohang University of Science and Technology, Pohang, Kyungpook, Korea

(Received 24 June 2002; accepted 28 August 2002)

We investigate rf transport through an AlGaAs/GaAs single-electron transistor (SET). The presented rf–SET scheme provides a transmission coefficient proportional to the admittance of the device, which is desirable for impedance analysis as well as for high-sensitivity charge detection. The impedance of a SET, including the small tunneling capacitance, is successfully analyzed at the high frequency of 643 MHz, and is compared with a simple model. The ability to measure the impedance of a SET would expand the measurable regime of single-electron tunneling behavior. © *2002 American Institute of Physics.* [DOI: 10.1063/1.1515883]

We discuss the radio-frequency single-electron transistor (rf–SET), which is a high-sensitivity and fast-response electrometer. The rf–SET is attractive for the detection of a single electron,[1,2] spin,[3] photon-absorption,[4] etc. Another interesting feature we focus on is the rf transport characteristics at a high frequency, f, of the $\sim$gigahertz domain. The rf–SET measurement provides information about the impedance of the device. A SET can be described by using two tunnel junctions characterized by tunneling resistance, R_t, and capacitance, C_t.[5] Usually, C_t is so small that it cannot be measured directly by a dc or low-frequency measurement. However, the impedance of the tunneling capacitance can be comparable to the tunneling resistance at a high frequency. Therefore, the impedance can be directly measured with an rf–SET. This letter presents the results of an impedance analysis of a SET and describes the interplay between the resistive and capacitive components of SET impedance.

We use a SET fabricated in an AlGaAs/GaAs two-dimensional electron system [see Fig. 1(a)].[6] The gate voltages, V_L and V_R, control the two tunneling barriers, and V_C is used to change the potential of the dot. We approximate this SET by using a simple circuit that consists of two tunneling junctions (characterized by R_{t1}, C_{t1}, R_{t2}, C_{t2}), other capacitances to ground (totally C_g, including all gate capacitances), and a stray capacitance between the two leads (C_s), as shown in Fig. 2(a). The stray capacitance is considered to account for our observations (see later). The charging energy of the dot is defined by $E_c = e^2/C_\Sigma$, where $C_\Sigma = C_{t1} + C_{t2} + C_g$. The conventional dc measurements, performed simultaneously with extra circuits (not shown in Fig. 1),[2] show clear Coulomb blockade (CB) oscillations with $E_c = 1-2$ meV (corresponding to $C_\Sigma = 0.08-0.16$ fF), and single-particle excitation spectra with the level spacing of $\Delta = 0.1-0.3$ meV.

We use a rf–SET circuit design to analyze the impedance [see Fig. 1(a)]. An input signal, $v_i e^{i\omega t}$, passes through a device and a resonator ($L_0 = 100$ nH, $C_0 \sim 0.6$ pF, the resonant frequency of $f = 643$ MHz, and the quality factor $Q \sim 8$), and the transmitted signal, $v_t e^{i\omega t}$, is investigated. Compared with reflection measurement, originally demonstrated by Schoelkopf,[1] and the transmission measurement with two inductors reported by us,[2] the present rf–SET circuit is the simplest. Moreover, the transmission coefficient, T, can be simplified as

$$T = v_t / v_i = -jQZ_0Y_X \tag{1}$$

under appropriate assumptions ($Q^2 \gg 1$ and $Q^2 Z_0 Y_X \ll 1$). Here, $Z_0 = 50\ \Omega$ is the impedance of the rf lines. Thus, T is simply proportional to the admittance of the investigated de-

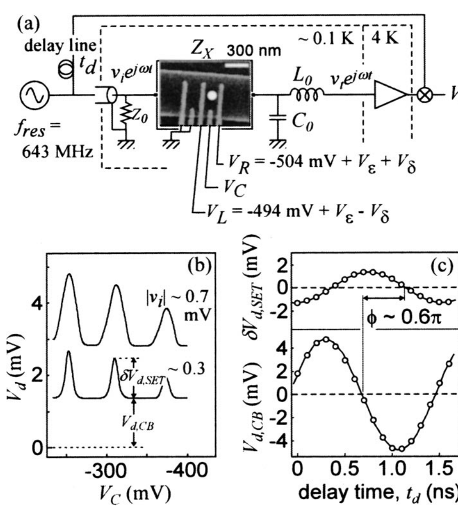

FIG. 1. (a) Schematic diagram of the measurement setup. The sample shown in the scanning electron micrograph contains a GaAs quantum dot (white circle) made by dry etching (upper and lower dark regions) and five Schottky gates (vertical bright lines). The measurement was done in a dilution refrigerator ($\sim$0.1 K). (b) Typical CB oscillations detected by the rf transmission signal at $t_d = 0.6$ ns. We analyze the detection amplitude in the CB region, $V_{d,\mathrm{CB}}$, and the peak height, $\delta V_{d,\mathrm{SET}}$. (c) Phase analysis of the transmission signal.

a)Also at: Pohang University of Science and Technology, Korea; present address: Keimyung University, Korea.
b)Author to whom correspondence should be addressed; electronic mail: fujisawa@will.brl.ntt.co.jp
c)Also at: CREST, 4-1-8 Honmachi, Kawaguchi 331-0012, Japan.

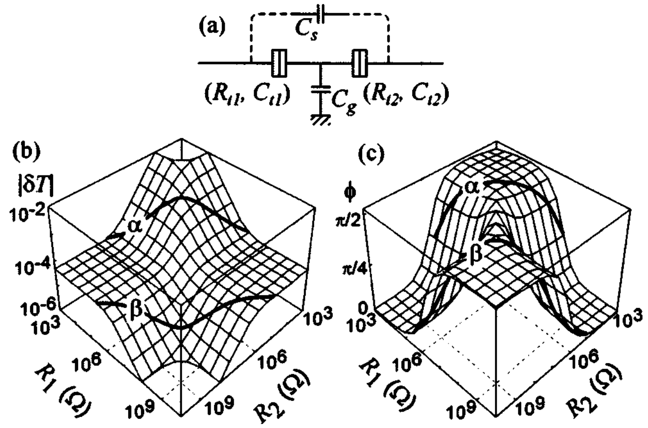

FIG. 2. (a) A simple model that describes a SET device with two tunneling barriers and capacitances. (b) and (c) The transmission coefficient, $|\delta T|$, and the phase, ϕ, of the SET peak measured relative to the CB region, using the simple model of (a) with $C_{t1}=C_{t2}=C_t=0.05$ fF, and $C_g=0.02$ fF. The thick lines, α and β, show typical behaviors, when V_δ is swept.

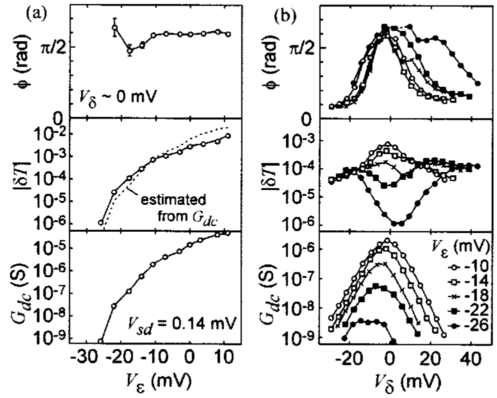

FIG. 3. The phase shift, ϕ, (upper panel), transmission coefficient, $|\delta T|$, (middle panel), and the dc conductance, $G_{\rm dc}$, (lower panel). The two gate voltages are swept simultaneously (a) in the same direction by V_ε, and (b) in the opposite direction by V_δ. For all data points, $V_C \sim -0.43$ V. The number of electrons in the dot increases by one with increasing V_ε by ~ 4 mV, while it is constant for the same V_ε in (b). The dashed line in the middle panel of (a) is the transmission coefficient calculated from $G_{\rm dc}$.

vice, Y_X (the inverse of the impedance, Z_X), while a small change from total reflection or total transmission has to be measured in the previous schemes.[1,2] These characteristics are suitable for the impedance analysis described later as well as for conventional charge-detection measurements. It should be noted that the frequency has to be fixed at the resonant frequency in the rf–SET scheme. Nevertheless, we can discuss the interesting interplay between resistance and capacitance components of the SET impedance by changing the tunneling resistance.

We apply a microwave carrier signal of the amplitude $|\nu_i| = 0.2$–0.7 mV at the resonant frequency. The excitation rf voltage applied across the SET is almost the same as $|\nu_i|$ in this scheme, while this is not the case for other schemes.[1,2] However, the charge sensitivity and bandwidth of the rf–SET should remain the same in principle.[7] The transmission signal is amplified and detected with a mixer (homodyne detection), which allows phase-sensitive measurement of the carrier rf signal.[2] The detected signal (a dc voltage), V_d, shows a sinusoidal dependence on the delay time, t_d, of the reference signal. We can obtain a complex value of T, and thus Y_X, from this dependence by using Eq. (1).

Figure 1(b) shows typical CB oscillations. The height and width of the peaks increase with $|\nu_i|$, and are actually affected by discrete energy states in the dot. However, the discrete energy levels are partially smeared out, since $|\nu_i|$ is comparable to or larger than the level spacing. In this work, we restrict ourselves to the classical CB regime to demonstrate the feasibility of impedance analysis using the rf–SET technique.

We start from an analysis in the CB region. Even in the CB region, V_d is a nonzero value, $V_{d,\rm CB}$, which changes sinusoidally with the delay time, t_d, as shown in Fig. 1(c). We can deduce this transmission coefficient $|T_{\rm CB}| = 7 \times 10^{-3}$ for this case. Since no electron tunneling is expected in the CB region ($R_{t1}=R_{t2}=\infty$), the admittance is approximately given by $Y_{X,\rm CB} \sim j\omega C_s$ for $C_s \gg C_\Sigma$ in the simple model. Thus, the phase of $V_{d,\rm CB}$ can be considered as a reference for the capacitive impedance. We obtained $C_s \sim 4$ fF in this device.

In contrast, the admittance of the SET is a complex value, $Y_{X,\rm SET}$, when the SET is conductive. For convenience, we analyzed the peak height, $\delta V_{d,\rm SET}$, rather than the absolute value. Since V_d is proportional to the admittance, the transmission through the stray capacitance does not contribute to the peak height. $\delta V_{d,\rm SET}$ also changes with t_d, accompanying with a phase shift, ϕ, from the $V_{d,\rm CB}$ trace [see Fig. 1(c)]. In principle, we can determine $\delta T = T - T_{\rm CB}$ and $\delta Y_{X,\rm SET} = Y_{X,\rm SET} - Y_{X,\rm CB}$ from this measurement. However, $\delta Y_{X,\rm SET}$ is a complicated function of the parameters of the simple model shown in Fig. 2(a). This can be written in a simple form in some specific cases. If the SET is made with two identical tunneling junctions ($R_{t1}=R_{t2}$ and $C_{t1}=C_{t2}$), $\delta Y_{X,\rm SET} \sim (R_{t1}+R_{t2})^{-1}$. In this case, the admittance is determined only by the tunneling resistances, and the rf–SET operation can be regarded as the "resistance mode." In contrast, if the two junctions are largely asymmetric ($\omega C_{t1} R_{t1} \ll 1 \ll \omega C_{t2} R_{t2}$), $\delta Y_{X,\rm SET} \sim j\omega C_{t2}(1 - C_{t1}/C_\Sigma)$. The admittance is only given by the capacitances (regarded as the "capacitance mode"). Their corresponding transmission amplitude, δT, can also be obtained by using Eq. (1). Figures 2(b) and 2(c) show numerical calculations of $|\delta T|$ and the argument of δT, ϕ, respectively, for the simple model with typical parameters of $C_{t1}=C_{t2}=0.05$ fF and $C_g=0.02$ fF. One can clearly identify the resistance mode, where $|\delta T|$ is sensitive to R_{t1} and R_{t2}, and $\phi \sim \pi/2$. The capacitance mode appears where $|\delta T|$ is insensitive to R_{t1} and R_{t2}, and $\phi \sim 0$. In the following, we demonstrate how well this simple model describes the realistic rf–SET operations.

In our device, we can almost independently control the tunneling resistances, R_{t1} and R_{t2}, with V_L and V_R, respectively, while C_{t1} and C_{t2} are expected to be almost constant. For convenience, we introduce two voltages; V_ε and V_δ, to change R_{t1} and R_{t2} simultaneously in the same direction (V_ε) or in the opposite direction (V_δ). They are defined by $V_L = -494\ \mathrm{mV} + V_\varepsilon - V_\delta$ and $V_R = -504\ \mathrm{mV} + V_\varepsilon + V_\delta$. The offset voltages were chosen so as to be symmetrical at $V_\varepsilon \sim V_\delta \sim 0$. Figure 3(a) shows the V_ε dependence at $V_\delta \sim 0$, where the tunneling resistances are kept almost same ($R_{t1} \sim R_{t2}$). $|\delta T|$ changes with V_ε in accordance with the dc conductance, $G_{\rm dc} = (R_{t1}+R_{t2})^{-1}$ [see the dashed lines in the

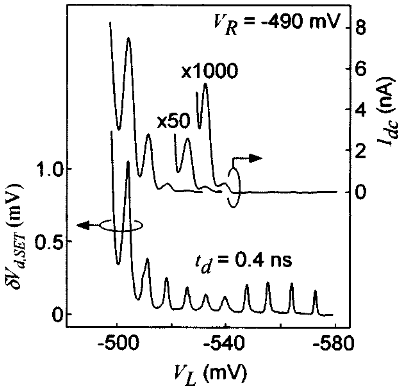

FIG. 4. CB oscillations measured by dc current (upper three traces) and by rf transmission (lower trace). $t_d = 0.4$ ns is adjusted at the highest sensitivity for the capacitance mode.

middle panel of Fig. 3(a)]. The phase shift, ϕ, is kept almost constant $\sim 0.6\pi$, which is close to $\pi/2$. These behaviors are consistent with the resistance mode. The consistency is observed in the wide range of G_{dc}, even if the frequency of electron tunneling, $G_{dc}|\nu_i|/e \sim 10$ MHz for $G_{dc} \sim 10^{-9}$ S, is smaller than the carrier frequency. The tunneling barriers can be approximated well by simple tunneling resistances even at this frequency.

Figure 3(b) shows the V_δ dependence obtained for several different V_ε, where the ratio R_{t1}/R_{t2} is largely changed. ϕ changes from $\sim 0.6\pi$ ($V_\delta \sim 0$) to $\sim 0.1\pi$ ($|V_\delta| > 20$ mV), indicating a transition from the resistance to the capacitance mode. $|\delta T|$ shows a peak or dip at $V_\delta \sim 0$, but becomes almost constant for $|V_\delta| > 20$ mV. These behaviors are consistent with the calculations in Fig. 2. Lines α and β are typical calculated traces, if R_1 and R_2 are swept logarithmically in the opposite directions. For instance, data at $V_\varepsilon = -10$ mV in Fig. 3(b) can be reproduced by using $C_{t1} = C_{t2} = 0.05$ fF. Since we know $C_\Sigma \sim 0.1$ fF from the charging energy ($E_C = 1.7$ meV) for this condition, the tunneling capacitances dominate the total capacitance and the charging energy.

There are some deviations from the simple model. We always observe ϕ in the 0.1π–0.6π range, while 0–0.5π, was expected in the model. The discrepancy might arise from unknown stray capacitances, inductances, or nonlinear behavior of the device.

Figure 4 shows CB oscillations when only V_L is swept. The dc current, I_{dc}, decreases dramatically with increasing R_{t1}, and fell below the noise level for $V_L < -540$ mV. However, CB oscillations are clearly identified in the capacitance mode of rf–SET. The peak height for $V_L < -520$ mV remains almost constant, implying that the junction capacitances do not change so much. We can resolve at least six additional peaks below $V_L < -580$ mV having similar peak heights. In principle, only one tunneling barrier is required for the capacitance mode of a rf–SET. This reminds us of capacitance spectroscopy, which successfully measures few-electron energy states in a vertical quantum disk.[8] The zero-electron state has been achieved in such vertical disk-shaped dots,[8,9] or in some well-designed lateral dots.[10,11] The capacitance mode of the rf–SET would be a useful tool for investigating the few-electron limit, since only one tunneling barrier is required.

In summary, we reported an impedance (admittance) analysis of a SET obtained by using rf transport. The transmission characteristics can be understood on the basis of a simple resistance and capacitance model. The feasibility of impedance analysis can be extended to other devices, especially when high-frequency impedance is essential.[5,12]

This work has partially been supported by the Ministry of Education of Korea through its BK21 program.

[1] R. J. Schoelkopf, P. Wahlgren, A. A. Kozhevnikov, P. Delsing, and D. E. Prober, Science **280**, 1238 (1998).

[2] T. Fujisawa and Y. Hirayama, Appl. Phys. Lett. **77**, 543 (2000).

[3] B. E. Kane, N. S. McAlpine, A. S. Dzurak, R. G. Clark, G. J. Milburn, He Bi Sun, and H. Wiseman, Phys. Rev. B **61**, 2961 (2000).

[4] S. Komiyama, O. Astafiev, V. Antonov, T. Kutsuwa, and H. Hirai, Nature (London) **403**, 405 (2000).

[5] *Single Charge Tunneling, Coulomb Blockade Phenomena in Nanostuctures*, NATO ASI series B 294, edited by H. Grabert and M. H. Devoret.

[6] L. P. Kouwenhoven C. M. Markus, P. L. McEuen, S. Tarucha, R. M. Westervelt, and N. S. Wingreen, in *Mesocopic Electron Transport*, NATO ASI series E 345, edited by L. L. Sohn, L. P. Kouwenhoven, and G. Schön, pp. 105–214.

[7] A. N. Korotkov and M. A. Paalanen, Appl. Phys. Lett. **74**, 4052 (1999).

[8] R. C. Ashoori, H. L. Stormer, J. S. Weiner, L. N. Pfeiffer, S. J. Pearton, K. W. Baldwin, and K. W. West, Phys. Rev. Lett. **68**, 3088 (1992).

[9] S. Tarucha, D. G. Austing, T. Honda, R. J. van der Hage, and L. P. Kouwenhoven, Phys. Rev. Lett. **77**, 3613 (1996).

[10] A. Fujiwara, Y. Takahashi, and K. Murase, Phys. Rev. Lett. **78**, 1532 (1997).

[11] M. Ciorga, A. S. Sachrajda, P. Hawrylak, C. Gould, P. Zawadzki, S. Jullian, Y. Feng, and Z. Wasilewski, Phys. Rev. B **61**, R16315 (2000).

[12] A. B. Zorin, S. V. Lotkhov, H. Zangerle, and J. Niemeyer, J. Appl. Phys. **88**, 2665 (2000).